Submitted: 31 May, 2022 Accepted: 04 August, 2022 Published: 15 December, 2022 DOI:10.22514/ejgo.2022.060

ORIGINAL RESEARCH

European Journal of Gynaecological Oncology

A prognostic signature of six necroptosis-related miRNAs for predicting the overall survival of breast cancer patients

Xiaohua Hong[1,†], Guangyao Wang[2,†], Zhen Rong[3,*], Wei Shi[2,*]

[1]Guangxi University of Chinese medicine, 530000 Nanning, Guangxi, China
[2]The First Affiliated Hospital of Guangxi University of Chinese Medicine, 530000 Nanning, Guangxi, China
[3]Bao'an Authentic TCM Therapy Hospital, 518100 Shenzhen, Guangdong, China

***Correspondence**
shiwei_doctor1980@163.com
(Wei Shi);
rongzhenw@163.com
(Zhen Rong)

† These authors contributed equally.

Abstract

Breast cancer (BRCA) is the most frequent malignant disease and cause of death in females. Recent studies have uncovered the crucial roles of necroptosis-related miRNAs in diverse cancers, including BRCA. However, the significance of necroptosis-related miRNA in predicting the prognosis of BRCA remains largely undefined. This study aimed at constructing a miRNA risk signature related to necroptosis and a nomogram for estimating the prognosis of BRCA. The miRNA expression data and related clinical information were downloaded from the BRCA cohort (containing tissue samples from BRCA patients and normal para-cancer patients) of The Cancer Genome Atlas (TCGA) database. We analyzed the miRNA expression profile and screened the differentially expressed necroptosis-related miRNAs between BRCA and non-tumor samples. Then, a risk signature for BRCA patients was developed based on prognostic necroptosis-related miRNAs. The prognostic value of the risk signature was determined by Cox regression analysis. We also constructed a prognostic nomogram based on risk signature and clinicopathological characteristics, and evaluated its clinical potential using a calibration chart. Lastly, to identify potential therapeutic target for BRCA. Six necroptosis-related miRNAs (miR-141-3p, miR-148a-3p, miR-200a-5p, miR-223-3p, miR-425-5p, miR-7-5p) were differentially expressed between normal and BRCA tissues, including five up-regulated miRNAs and one down-regulated miRNA. They were used to construct the risk signature. Receiver Operating Characteristic (ROC) curve analysis indicated that the risk signature had good sensitivity and specificity (2-year area under curve (AUC): 0.627; 3-year AUC: 0.647) and was an independent prognostic factor (univariate Cox regression: hazard ratio (HR) = 1.8066, 95% confidence interval (CI) (1.2867–2.5365), $p < 0.05$; multivariate Cox regression: HR = 1.5246, 95% CI (1.0830–2.1462), $p < 0.05$). Calibration chart showed that the nomogram had good accuracy for predicting the prognosis of BRCA patients. We also identified miR-223a-3p as a potential therapeutic target for BRCA. This study identified 6 promising necroptosis-related miRNAs, which were used to construct a signature model to predict BRCA patients' prognosis. Further, a nomogram based on risk signatures and clinicopathological characteristics was constructed and showed promising potential as an effective and individualized diagnostic tool.

Keywords

Breast cancer; Necroptosis; Risk signature; Prognostic prediction; Survival

1. Introduction

Breast cancer (BRCA) is a highly heterogeneous and aggressive malignant disease [1]. It has currently surpassed lung cancer as the most frequently occurring cancer worldwide and is also the most frequently diagnosed and cause of cancer-related death in females [2]. BRCA patients from high-risk regions or countries (the United States, Denmark, Ireland, *etc.*) have shown good responses to therapies, leading to a decrease in mortality rates [3–5], with the 5-year survival rate of BRCA patients being as low as 12%–20% in some countries [6]. However, the incidence and mortality of BRCA in regions such as South America, Asia and Africa are still increasing annually. Due to the high heterogeneity of BRCA, remarkable differences have been observed in the etiology, pathological manifestations, and therapeutic response of the patients, leading to huge challenges for improving the outcomes of BRCA. With in-depth molecular mechanism and genomics exploration, the heterogeneity of BRCA and its underlying mechanism of carcinogenesis have been gradually unveiled, with

This is an open access article under the CC BY 4.0 license (https://creativecommons.org/licenses/by/4.0/).
 ©2022 The Author(s). Published by MRE Press.

several therapeutic targets and prognostic markers identified. For instance, due to the significant benefits from tamoxifen and trastuzumab, which target estrogen receptor (ER) and human epidermal growth factor receptor-2 (HER2), they are widely used for BRCA treatment [7]. However, despite these promising responses, many patients still experience drug resistance, tumor progression and metastasis, which greatly affects their treatment outcomes and quality of life. Therefore, identifying effective treatment targets and prognostic markers, developing risk prediction models and improving individualized treatment modalities are essential to improve therapeutic efficacy and prognosis.

Necroptosis, a new form of programmed death with mixed characteristics of cell necrosis and apoptosis, is distinct from cell necrosis and apoptosis, despite showing similarities with necrosis in morphology and apoptosis in mechanism [8]. Necroptosis can be evoked by diverse stimuli, including viral infection, tumor necrosis factor, *etc.*, and is pathologically characterized by cell swelling, membrane perforation, rupture and incompleteness, and severe inflammation, but without significant change in chromatin [9]. The inductive mechanism of necroptosis is related to the activation of a battery of kinases. The activated receptor-interacting protein kinase (RIPK) 1 and RIPK3 phosphorylate mixed-lineage kinase domain-like pseudokinase (MLKL) can form necroptotic bodies, leading to necroptosis [10, 11]. Necroptosis has been shown to facilitate the progression and metastasis of malignancies by controlling key regulators and delay cancer progression when damage or resistance to apoptosis occurs [12, 13]. Thus, considering its anti-tumor effects and good performance in drug-resistant BRCA and triple-negative BRCA [14–16], necroptosis is an appealing target for BRCA treatment.

MicroRNAs (miRNAs) are a set of short non-coding RNA with regulatory functions, which not only regulate mRNA expression but also target non-coding RNAs (long non-coding RNAs and miRNAs) [17]. Researchers have found that miRNA regulates many biological processes, including human body development and cell stability, by influencing gene expression [18, 19]. There is also increasing evidence showing miRNAs regulating biological processes such as proliferation, adhesion, inflammation, senescence, and apoptosis [20]. Consequently, anomalies in miRNAs can lead to many diseases. Several studies have identified abnormal miRNAs in cancer, while disturbances in their biological processes such as proliferation, adhesion and inflammation have been associated with cancer development, indicating their vital modulatory role in human cancer [21, 22].

MiRNAs also exert tumor suppressor or oncogenic effects, influencing malignant BRCA occurrence and progression [23]. Tang *et al.* [24] found that the down-regulation of miR-200 family members, such as miR-200a and miR-141, led to high expression of friend leukaemia integration-1 (FLI1) and transcription factor 12 (TCF12) and BRCA invasion and metastasis. Kong *et al.* [25] reported that the down-regulation of miR-7 and upregulation of focal adhesion kinase (FAK), which is usually directly targeted by miR-7, was correlated with the invasive phenotype of BRCA in metastatic BRCA patients. However, there is limited data on the prognostic effect of necroptosis-related miRNAs in BRCA.

Based on the existing findings and limitations in current literature, this study mainly focused on investigating the prognostic value of necroptotic miRNAs in BRCA to identify effective therapeutic targets and prognostic markers by developing risk signature-based models. Further, we assessed the clinicopathological factors of BRCA patients to develop a nomogram for estimating individual risk [26] and also developed a prognostic nomogram incorporating clinical factors and necroptotic miRNA risk signature to evaluate the clinical prognosis of BRCA patients.

2. Materials and methods

2.1 Data retrieval

The BRCA miR-seq transcriptome data were primarily downloaded and sorted through The Cancer Genome Atlas (TCGA) (https://portal.gdc.cancer.gov/) public database, from which we obtained sample data and corresponding clinical information of 1103 BRCA and 104 normal cases. As the relevant data in the TCGA database are publicly available, we strictly abided by the data access policy of the TCGA database and ethical approval for this study was not required. For identifying the necroptotic miRNAs, we mainly referred to the investigations of Liu *et al.* [12], from which 13 miRNAs related to necroptosis, namely miR-495, miR-331-3p, miR-15a, miR-148a-3p, miR-7-5p, miR-141-3p, miR-425-5p, miR-200a-5p, miR-210, miR-223-3p, miR-500a-3p, miR-181-5p and miR-16-5p, were retrieved.

2.2 Identification of necroptotic miRNAs differentially expressed between tumor and normal tissues

Before differential analysis, data matching for the 13 necroptotic miRNAs with the obtained TCGA cohort was performed utilizing the “tidyverse” package in R language software (4.1.0, Ross Bell Laboratories, Vienna, Austria), followed by data normalization. Then, the “limma” package was utilized to identify differentially expressed necroptotic miRNAs between BRCA tissues and normal tissues, using a false discovery rate (FDR) <0.05 as the criterion.

2.3 Prognostic models of necroptosis-related miRNAs

To assess the prognostic value of necroptotic miRNAs, Cox regression analysis was performed to identify the necroptotic miRNAs closely associated with the overall survival (OS) of BRCA patients, based on which 6 survival-related necroptotic miRNAs were identified. Since the number of necroptotic miRNAs obtained was less than 10, the Least absolute shrinkage and selection operator (LASSO) regression model was not utilized for further analysis. Next, risk characteristic models were constructed for the 6 survival-related necroptotic miRNAs. The risk score of each BRCA patient was expressed by the sum of the retained scores of the necroptotic miRNAs. The score of each necroptotic miRNA was calculated by multi-

TABLE 1. Clinical characteristics of the BRCA patients used in this study.

Characteristics	Alive (n = 926)	Dead (n = 150)	Total (n = 1076)	*p*-value	FDR
Cancer type					
Breast cancer	926 (86.06%)	150 (13.94%)	1076 (100.00%)		
Survival time (OS)					
Mean ± SD	1201.17 ± 1161.43	1595.35 ± 1309.80	1256.12 ± 1190.44		
Age					
≤65	682 (63.38%)	91 (8.46%)	773 (71.84%)	1.50×10^{-3}	2.90×10^{-3}
>65	244 (22.68%)	59 (5.48%)	303 (28.16%)		
Gender					
Female	915 (85.04%)	149 (13.85%)	1064 (98.88%)	0.88	0.88
Male	11 (1.02%)	1 (0.09%)	12 (1.12%)		
Stage					
Stage I	167 (15.52%)	16 (1.49%)	183 (17.01%)		
Stage II	543 (50.46%)	65 (6.04%)	608 (56.51%)		
Stage III	198 (18.40%)	44 (4.09%)	242 (22.49%)	1.70×10^{-18}	1.00×10^{-17}
Stage IV	5 (0.46%)	15 (1.39%)	20 (1.86%)		
Stage X	6 (0.56%)	6 (0.56%)	12 (1.12%)		
NA	7 (0.65%)	4 (0.37%)	11 (1.02%)		
T					
T1	248 (23.05%)	33 (3.07%)	281 (26.12%)		
T2	545 (50.65%)	76 (7.06%)	621 (57.71%)		
T3	108 (10.04%)	25 (2.32%)	133 (12.36%)	2.10×10^{-5}	6.40×10^{-5}
T4	23 (2.14%)	15 (1.39%)	38 (3.53%)		
TX	2 (0.19%)	1 (0.09%)	3 (0.28%)		
N					
N0	460 (42.75%)	44 (4.09%)	504 (46.84%)		
N1	301 (27.97%)	60 (5.58%)	361 (33.55%)		
N2	98 (9.11%)	22 (2.04%)	120 (11.15%)	5.40×10^{-8}	2.20×10^{-7}
N3	59 (5.48%)	15 (1.39%)	74 (6.88%)		
NX	8 (0.74%)	9 (0.84%)	17 (1.58%)		
M					
M0	775 (72.03%)	120 (11.15%)	895 (83.18%)		
M1	5 (0.46%)	17 (1.58%)	22 (2.04%)	1.10×10^{-17}	5.30×10^{-17}
MX	146 (13.57%)	13 (1.21%)	159 (14.78%)		

FDR: false discovery rate; OS: overall survival; SD: standard deviation; NA: not available.

TABLE 2. Time-dependent-Roc curve estimated using IPCW.

Year	Cases	Survivors	Censored	AUC (%)
t = 2	42	583	431	62.69
t = 3	69	426	561	64.66

AUC: area under curve.

plying the miRNA coefficient by the miRNA expression level utilizing the following formula:

Risk score = $\sum_{i=1}^{n} coefi \times expi$, wherein n refers to the number of miRNAs, coefi refers to the regression coefficient of miRNA, and expi refers to the expression level of miRNA [27, 28]. Then, the BRCA cases were assigned to a low-risk and a high-risk group based on the strength of the median risk score. The "survival", "timeROC", and "ROCR" packages were used to compare the OS between the low- and high-risk groups, followed by receiver operating characteristic (ROC) curve analysis. The time-dependent ROC curve was based on the area under the ROC curve (AUC) to evaluate the prognostic value of the biomarkers [29]. In this study, AUC values ranged from 0 to 1, with an AUC of 0.5 indicating that the model has no predictive value and AUC of 0.5–1 indicating superior to random guesses and potential predictability [30, 31]. Univariate and multivariate Cox regression analyses were also performed to determine whether the risk features could serve as an independent biomarker of OS in BRCA.

2.4 Construction of a predictive nomogram

A clinical prognostic nomogram was plotted utilizing the "survival" and "rms" R packages, which covered the overall survival (OS)-associated risk signature and clinical factors involving age and tumor-node-metastasis (TNM) staging of BRCA patients. The *p* values, hazard ratio (HR) values, and 95% confidence interval (CI) of the risk signature and clinical factors are displayed in a forest plot, built using the "forestplot" package. The "pheatmap" package was used to plot a heat map of risk signature and related clinical factors. Next, a calibration curve was drawn to evaluate the consistency between the predicted results based on a prediction nomogram and the actual clinical results.

2.5 Function analysis

The survival curves of the six prognostic necroptosis-related miRNAs were analyzed utilizing the "survival" package of the R language software. Furthermore, the necroptosis-related miRNAs were screened with a threshold of $p < 0.05$. Three online databases miRDB, miRTarBase and TargetScan (http://www.mirdb.org/; http://mirtarbase.mBRCA.nctu.edu.tw/php/index.php; http://www.targetscan.org) were utilized for predicting the potential target genes of the miRNA candidates ($p < 0.05$). The "VennDiagram" package was employed to plot a Venn diagram showing the intersection among the targets gained from three databases, and the Cytoscape software (v3.8.0) was adopted to visualize the mRNA-miRNA regulatory network. Lastly, Gene Ontology (GO) and Kyoto Encyclopedia of Genes and Genomes (KEGG) analyses were performed to identify target gene candidates using the "org.Hs.eg.db" R package, the "clusterProfiler" R package [32], the "enrichplot" R package, and the "ggplot2" R package.

3. Results

3.1 Basic Information

The flow diagram of this study is shown in Fig. 1. The BRCA cohort and related clinical information were downloaded from the TCGA database, and sample data were obtained for 1103 BRCA patients and 104 normal controls. The data of 1076 BRCA and 104 normal samples were used for this study after excluding 27 BRCA samples due to missing clinical information. The detailed clinical characteristics of 1076 BRCA patients are summarized in Table 1.

3.2 Necroptosis-related miRNAs differentially expressed between tumor and non-tumor tissues

Six differentially expressed necroptotic miRNAs were identified between the tumor and non-tumor tissues, consisting of 5 up-regulated miRNAs (miR-141-3p, miR-148a-3p, miR-200a-5p, miR-425-5p, and miR-7-5p) and 1 down-regulated miRNA (miR-223-3p). The expression patterns of the differentially expressed miRNAs are displayed in the heat map of Fig. 2, wherein the rows represent the miRNAs and columns represent biological samples, with high expression indicated in red and low expression in green.

3.3 Prognostic models of the 6 necroptotic miRNAs

Here, Cox regression analysis was performed to identify necroptotic miRNAs correlated with the OS of BRCA patients and ultimately, the 6 necroptotic miRNAs were incorporated into the risk characteristic models. The patient's risk score was calculated using the following formula: (−0.29911 × miR-141-3p) + (0.08017 × miR-148a-3p) + (−0.11211 × miR-200a-5p) + (−0.48988 × miR-223-3p) + (−0.04474 × miR-425-5p) + (0.14614 × miR-7-5p). Using the median risk score as threshold (Fig. 3A, low-risk is represented by a solid blue line, and high-risk is represented by a solid red line), the BRCA patients were classified into a low- and high-risk group (n = 528 for each cohort). The patient survival status of each group is shown in Fig. 3B, in which the low-risk group is presented on the left side and the high-risk on the right side of the dotted line. In total, 82 deaths occurred in the high-risk cohort, while the low-risk cohort exhibited fewer deaths (n = 64) and superior OS (Fig. 3C, $p = 0.001$). The sensitivity and specificity of the prognostic model constructed by the 6 necroptotic miRNAs were assessed by ROC curve analysis. The AUC for 2-year and 3-year OS was 0.627 and 0.647, respectively (Fig. 3D, Table 2).

3.4 The prognostic values of the risk signature

Univariate and multivariate Cox regression analyses were performed to determine whether the risk signature of the 6 necroptotic miRNAs could serve as independent prognostic factors in the BRCA cohort. Univariate analysis showed the risk signature concerning the 6 necroptotic miRNAs was a significant prognostic factor in the BRCA cohort (HR = 1.8066, 95% CI (1.2867–2.5365), $p < 0.05$; Fig. 4A). After integrating other complex factors, it was determined to be an independent

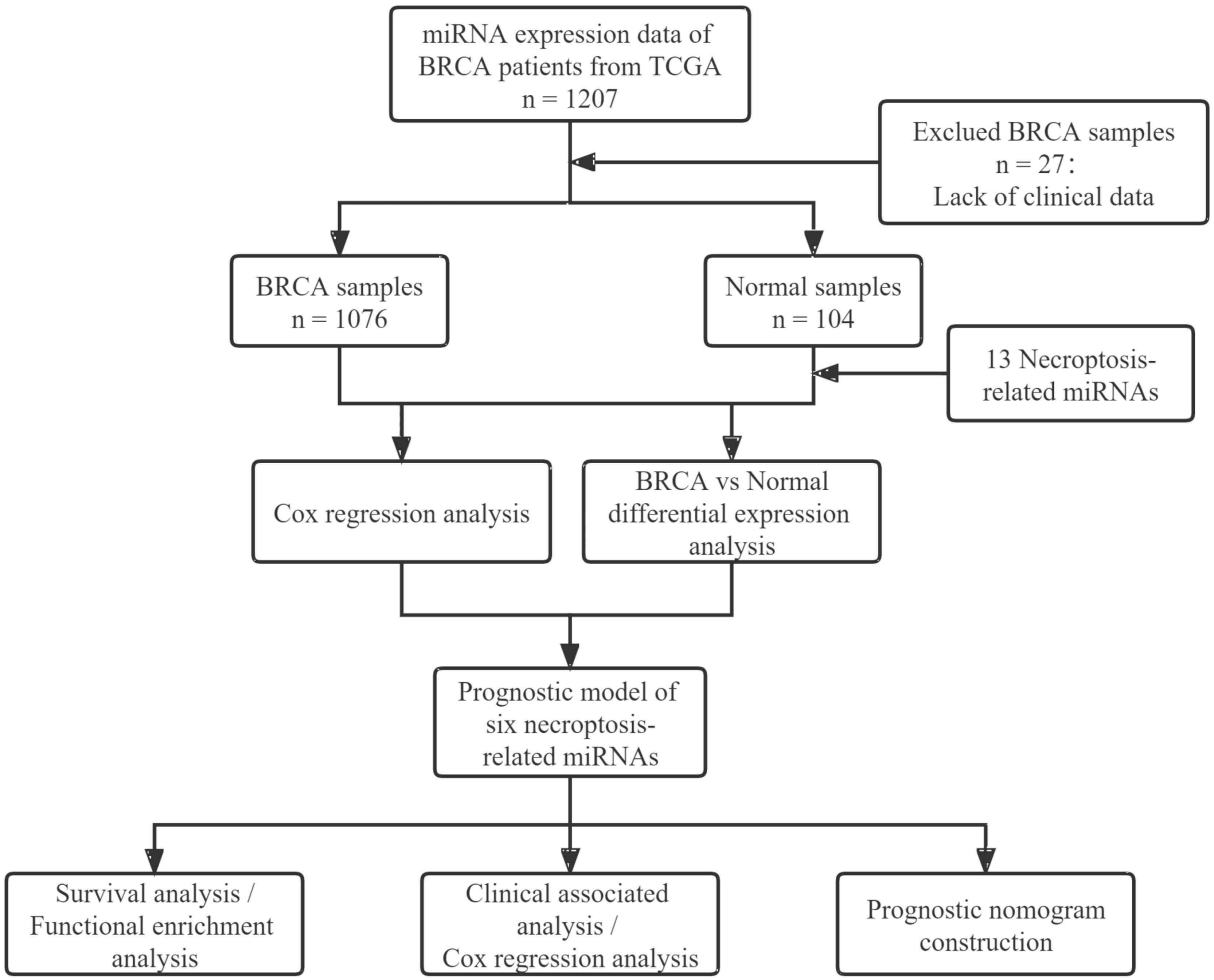

FIGURE 1. Flow diagram. BRCA: breast cancer; TCGA: The Cancer Genome Atlas.

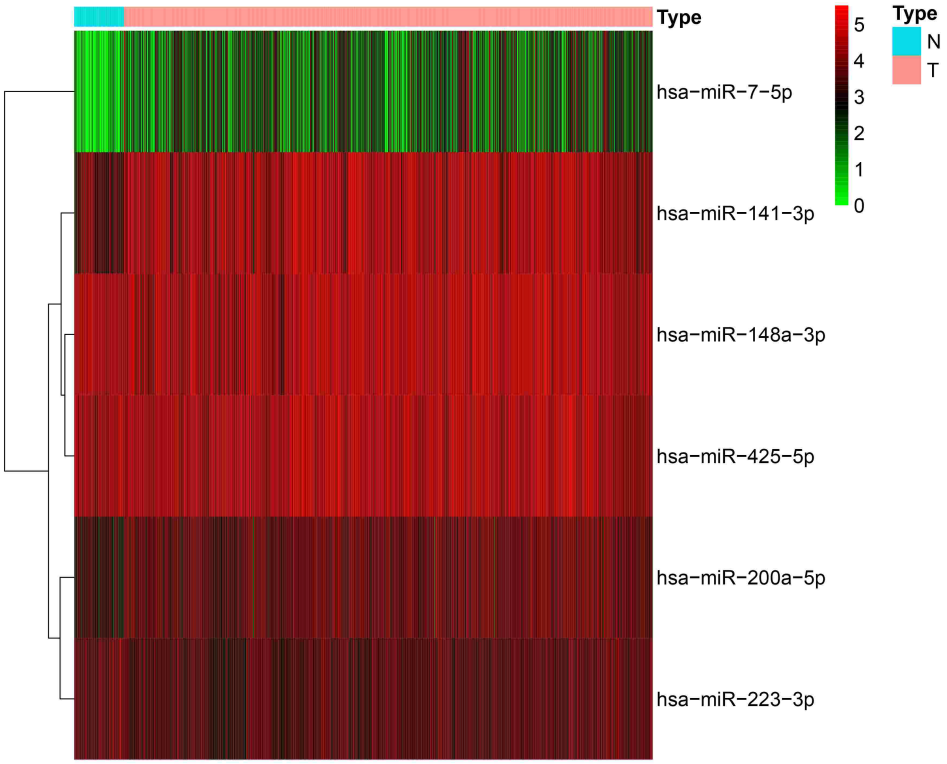

FIGURE 2. The heatmap of 6 differentially expressed necroptotic miRNAs.

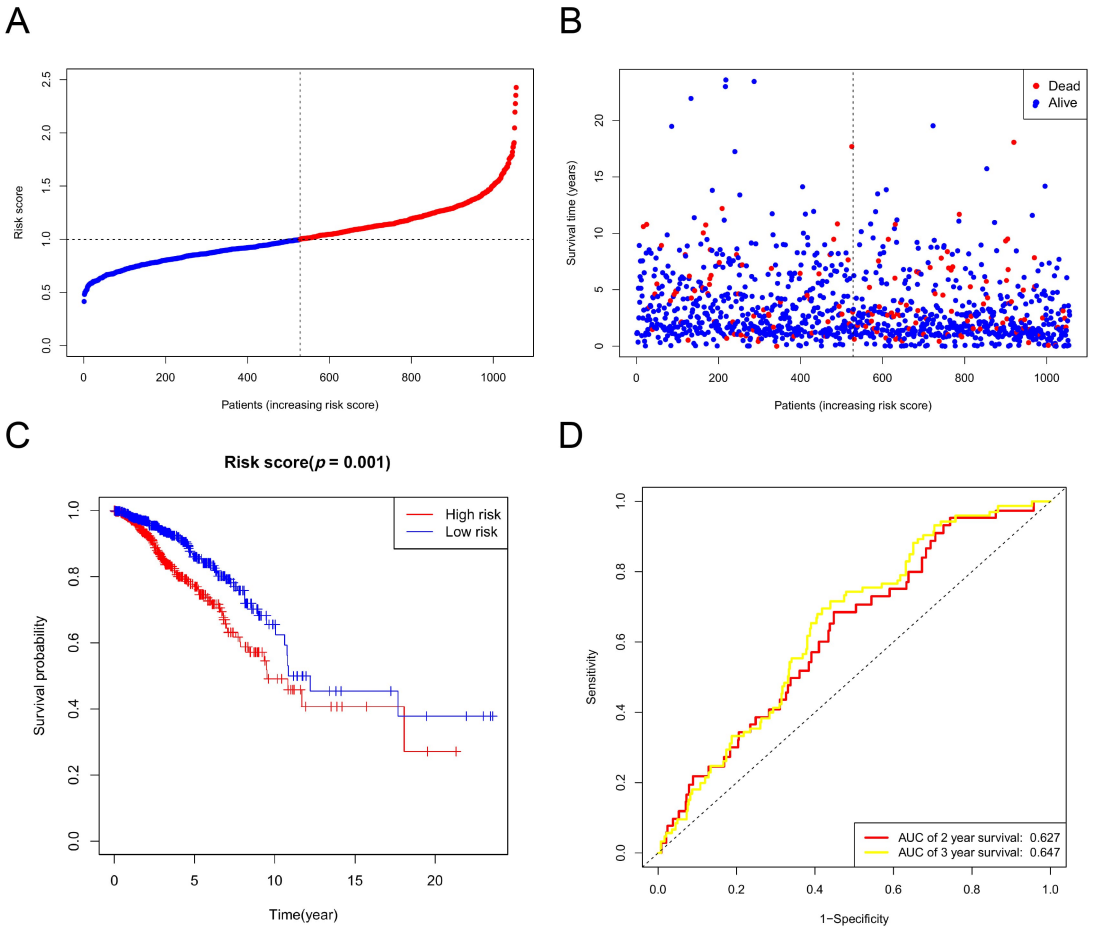

FIGURE 3. Prognostic models of 6 necroptotic miRNAs. (A) Distribution of patients in the low- and high-risk cohorts. (B) OS of patients in the low- and high-risk cohorts. (C) Survival curves of patients in the low- and high-risk cohorts. (D) ROC curves showing the predictive value of the prognostic model based on the 6 necroptotic miRNAs. AUC: area under curve.

prognostic factor for BRCA in the multivariate analysis (HR = 1.5246, 95% CI (1.0830–2.1462), $p < 0.05$; Fig. 4B). Furthermore, the 6 necroptotic miRNAs expression and clinical features of BRCA patients also showed differences between the two risk group (Fig. 4C).

3.5 Nomograms based on risk signature and clinicopathological characteristics

The risk signature and clinicopathological characteristics (age and TNM stage) were used to build a nomogram for predicting the 3- and 5-year OS of BRCA patients. We calculated the score value of each corresponding factor on the scale based on the condition of each individual to generate a total score for each patient (Fig. 5A). Then, the performance of the nomogram was evaluated by a calibration chart. An ideal prediction is represented by a solid blue line, and an actual prediction is represented by a solid red line. A nomogram is more accurate when the red and blue solid lines are closer [33]. The calibration chart of the constructed nomogram showed that the solid red line was close to the solid blue line, demonstrating good performance in predicting the 3- and 5-year OS of BRCA patients and in line with clinical practice (Fig. 5B–C).

3.6 Functional significance and potential mechanism of miR-223-3p in BRCA

Kaplan-Meier survival curve shows that BRCA patients with low miRNA-223-3p expression had significantly worse prognoses (Fig. 6A). The potential target genes of miR-223-3p were predicted utilizing three online databases (miRDB, miRTarBase, and TargetScan) and 30 overlapping genes, which can be visualized in the Venn diagram. The miRNA-mRNA regulatory network can be visualized in Fig. 6B–C. To further understand the functions of the 30 potential target genes, we performed GO and KEGG pathway enrichment analyses. The most reliable biological processes, molecular functions, and enriched pathways were screened based on the *p*-value (Fig. 7A–B). Among them, we found that these genes were mainly enriched in the MAPK (mitogen-activated protein kinase) signaling pathway, signaling pathways regulating pluripotency of stem cells, and transcriptional misregulation in cancer. Additionally, miR-223-3p target genes were found to primarily correlate with tumor cell proliferative, migratory and invasive processes, modulation of stem cell pluripotency, cancer transcription, *etc.* (Table 3).

TABLE 3. The miR-223-3p target genes and their functional analysis.

GO/KEGG	ID	Description	*p*-value	*p*. adjust	Target genes
BP	GO: 0001779	Natural killer cell differentiation	6.62×10^{-6}	0.006164	NLRP3, RIF1, RRAS2
BP	GO: 0043502	Regulation of muscle adaptation	1.52×10^{-5}	0.006164	FOXO1, FOXO3, IL6ST, SEPT2
BP	GO: 0070301	Cellular response to hydrogen peroxide	1.52×10^{-5}	0.006164	ECT2, FOXO1, FOXO3, PHF19
BP	GO: 1903706	Regulation of hemopoiesis	1.77×10^{-5}	0.006164	FBXW7, FOXO3, MEF2C, NLRP3, RRAS2, TOX
BP	GO: 0043500	Muscle adaptation	3.48×10^{-5}	0.007696	FOXO1, FOXO3, IL6ST, SEPT2
BP	GO: 0002066	Columnar/cuboidal epithelial cell development	4.24×10^{-5}	0.007696	IL6ST, NLRP3, TWF1
BP	GO: 0042593	Glucose homeostasis	4.33×10^{-5}	0.007696	CFTR, FOXO1, FOXO3, IGF1R, TWF1
BP	GO: 0033500	Carbohydrate homeostasis	4.41×10^{-5}	0.007696	CFTR, FOXO1, FOXO3, IGF1R, TWF1
BP	GO: 0042542	Response to hydrogen peroxide	7.24×10^{-5}	0.010187	ECT2, FOXO1, FOXO3, PHF19
BP	GO: 0034599	Cellular response to oxidative stress	7.30×10^{-5}	0.010187	ECT2, FBXW7, FOXO1, FOXO3, PHF19
MF	GO: 0001221	Transcription coregulator binding	0.000249	0.031019	FOXO1, FOXO3, LMO2
MF	GO: 0001228	DNA-binding transcription activator activity, RNA polymerase II-specific	0.000631	0.031019	FOXO1, FOXO3, MEF2C, NFIA, TWF1
MF	GO: 0001216	DNA-binding transcription activator activity	0.000669	0.031019	FOXO1, FOXO3, MEF2C, NFIA, TWF1
MF	GO: 0001227	DNA-binding transcription repressor activity, RNA polymerase II-specific	0.001355	0.038670	FOXO3, NLRP3, RIF1, TWF1
MF	GO: 0001217	DNA-binding transcription repressor activity	0.001403	0.038670	FOXO3, NLRP3, RIF1, TWF1
MF	GO: 0019903	Protein phosphatase binding	0.001669	0.038670	CDC27, FOXO1, HSP90B1
KEGG	hsa04152	AMPK signaling pathway	0.000120	0.009319	CFTR, FOXO1, FOXO3, IGF1R
KEGG	hsa04550	Signaling pathways regulating pluripotency of stem cells	0.000235	0.009319	IGF1R, IL6ST, POLR3G, TWF1
KEGG	hsa04213	Longevity regulating pathway-multiple species	0.000321	0.009319	FOXO1, FOXO3, IGF1R
KEGG	hsa05202	Transcriptional misregulation in cancer	0.000722	0.015705	FOXO1, IGF1R, LMO2, MEF2C
KEGG	hsa04211	Longevity regulating pathway	0.000929	0.016170	FOXO1, FOXO3, IGF1R
KEGG	hsa05215	Prostate cancer	0.001193	0.017301	FOXO1, HSP90B1, IGF1R

GO: Gene Ontology; KEGG: Kyoto Encyclopedia of Genes and Genomes; ID: Identification; BP: Biological Process; MF: Molecular Function; AMPK: Adenosine 5'-monophosphate (AMP)-activated protein kinase; NLRP3: NOD-like receptor thermal protein domain associated protein 3; RIF1: Replication Timing Regulatory Factor 1; RRAS2: RAS Related 2; FOXO1: Forkhead Box O1; FOXO3: Forkhead Box O3; IL6ST: Interleukin 6 Cytokine Family Signal Transducer; SEPT2: Septin 2; ECT2: Epithelial Cell Transforming 2; PHF19: PHD Finger Protein 19; FBXW7: F-Box And WD Repeat Domain Containing 7; MEF2C: Myocyte Enhancer Factor 2C; TOX: Thymocyte Selection Associated High Mobility Group Box; TWF1: Twinfilin Actin Binding Protein 1; CFTR: CF Transmembrane Conductance Regulator; IGF1R: Insulin Like Growth Factor 1 Receptor; PHF19: PHD Finger Protein 19; LMO2: LIM Domain Only 2; NFIA: Nuclear Factor I A; CDC27: Cell Division Cycle 27; HSP90B1: Heat Shock Protein 90 Beta Family Member 1; POLR3G: RNA Polymerase III Subunit G.

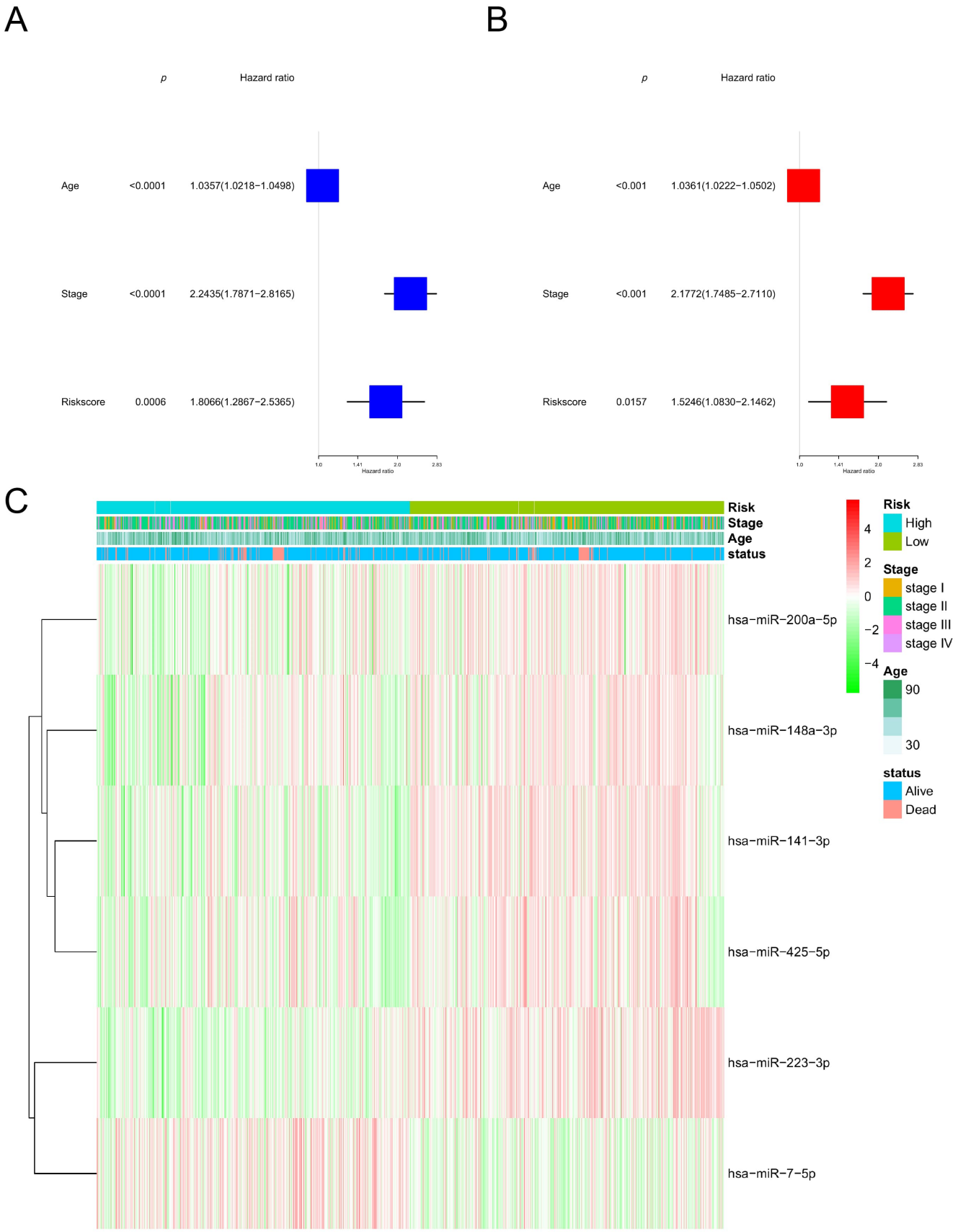

FIGURE 4. The risk signature was identified as an independent prognostic factor in the BRCA cohort. (A) Results of univariate Cox regression analysis in the BRCA cohort. (B) Results of multivariate Cox regression analysis in the BRCA cohort. (C) Heatmap of clinicopathological characteristics of the low- and high-risk populations.

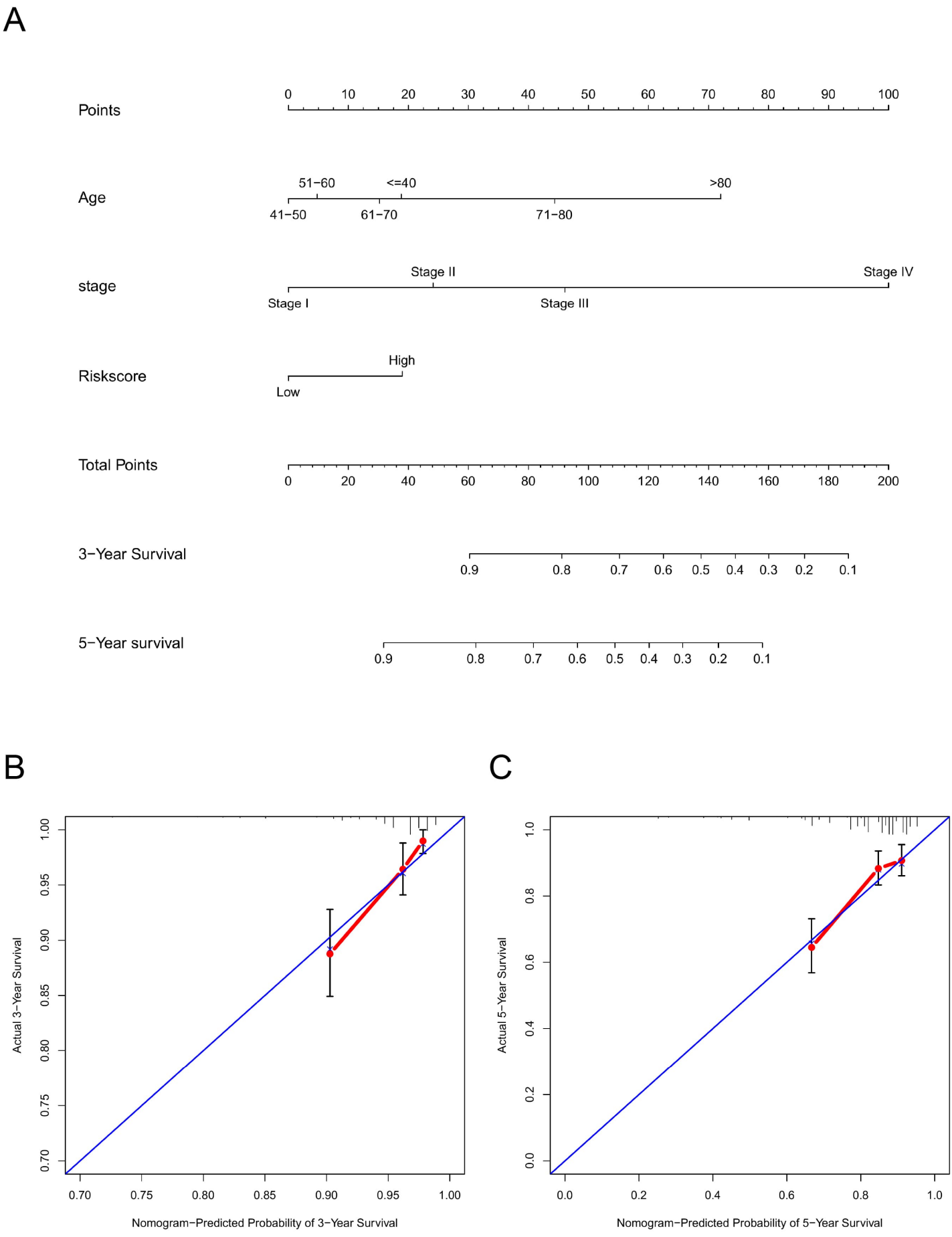

FIGURE 5. Prognostic nomogram based on the incorporated risk signature and clinicopathological characteristics. (A) Nomogram for the 3- and 5-year OS of BRCA patients. (B) Calibration chart of the nomogram for predicting the 3-year OS of BRCA patients. (C) A Calibration chart of the nomogram for predicting the 5-year OS of BRCA patients.

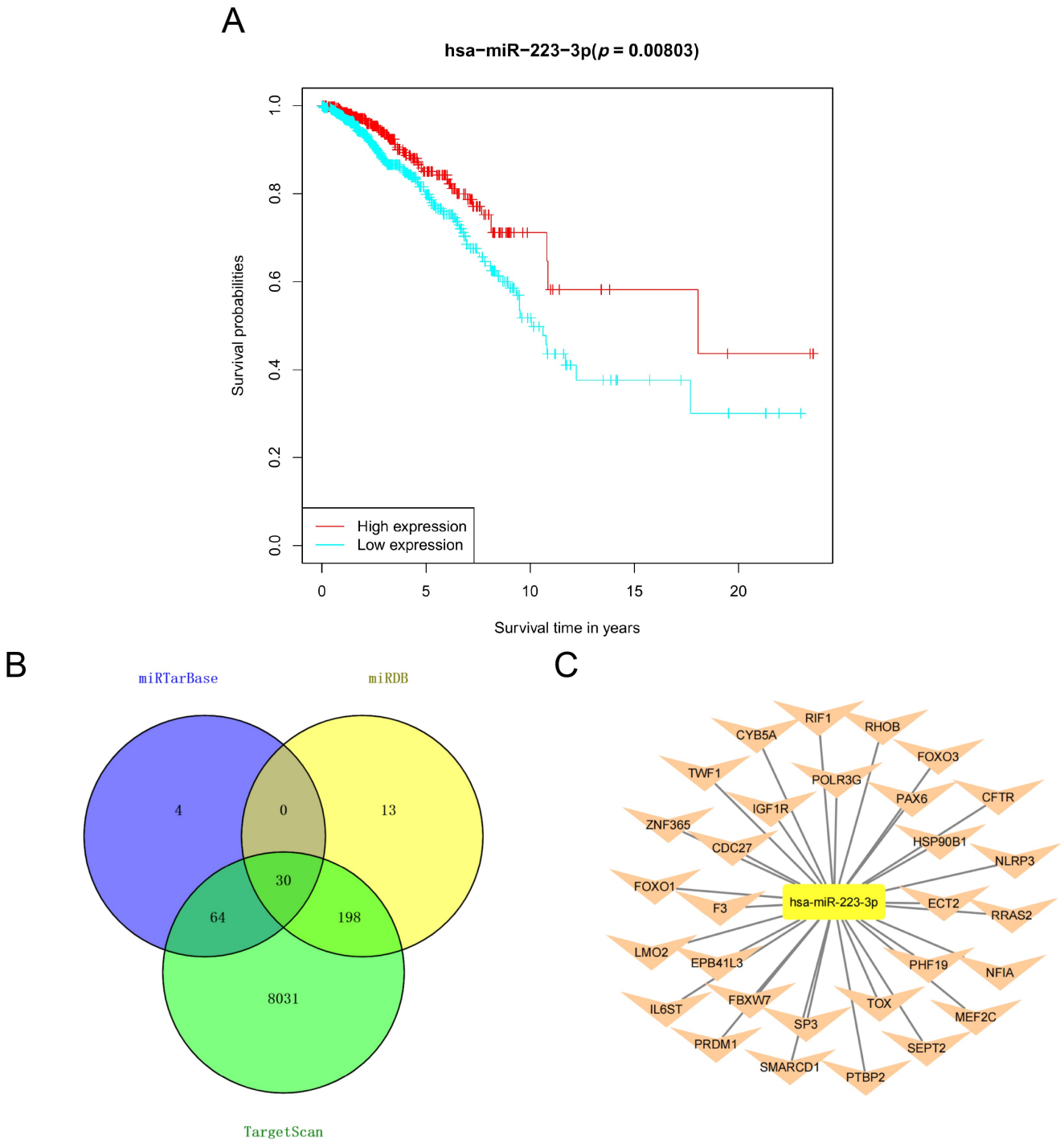

FIGURE 6. Functional analysis of miR-223-3p. (A) Patients with low miR-223-3p expression are associated with poor prognoses. (B) Intersected targets of miR-223-3p predicted by miRDB, miRTarBase and TargetScan databases. (C) The miRNA-mRNA regulatory network. CDC27: Cell Division Cycle 27; CFTR: CF Transmembrane Conductance Regulator; CYB5A: Cytochrome B5 Type A; ECT2: Epithelial Cell Transforming 2; EPB41L3: Erythrocyte Membrane Protein Band 4.1 Like 3; F3: Coagulation Factor III, Tissue Factor; FBXW7: F-Box And WD Repeat Domain Containing 7; FOXO1: Forkhead Box O1; FOXO3: Forkhead Box O3; HSP90B1: Heat Shock Protein 90 Beta Family Member 1; IGF1R: Insulin Like Growth Factor 1 Receptor; IL6ST: Interleukin 6 Cytokine Family Signal Transducer; LMO2: LIM Domain Only 2; MEF2C: Myocyte Enhancer Factor 2C; POLR3G: RNA Polymerase III Subunit G; PRDM1: PR/SET Domain 1; PTBP2: Polypyrimidine Tract Binding Protein 2; RHOB: Ras Homolog Family Member B; RIF1: Replication Timing Regulatory Factor 1; RRAS2: RAS Related 2; SEPT2: Septin 2; SMARCD1: SWI/SNF Related, Matrix Associated, Actin Dependent Regulator Of Chromatin, Subfamily D, Member 1; SP3: Sp3 Transcription Factor; TOX: Thymocyte Selection Associated High Mobility Group Box; TWF1: Twinfilin Actin Binding Protein 1; ZNF365: Zinc Finger Protein 365; NFIA: Nuclear Factor I A; NLRP3: NOD-like receptor thermal protein domain associated protein 3; PAX6: Paired Box 6; PHF19: PHD Finger Protein 19.

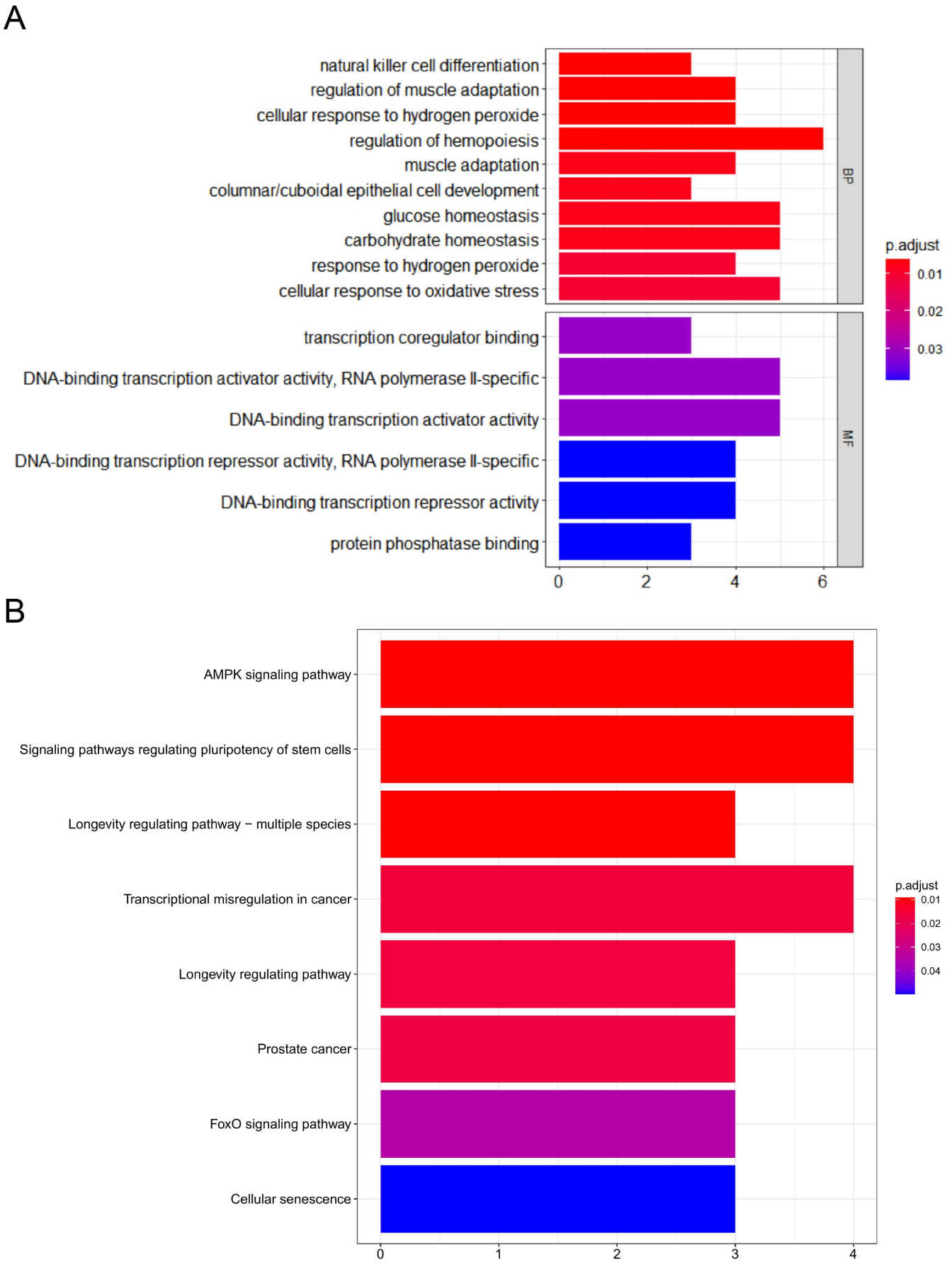

FIGURE 7. GO and KEGG pathway enrichment results. (A) GO enrichment analysis results. (B) KEGG pathway enrichment results. BP: Biological Process; MF: Molecular Function; AMPK: Adenosine 5'-monophosphate (AMP)-activated protein kinase; FOXO: Forkhead Box O.

4. Discussion

BRCA is associated with high global morbidity and mortality, indicating an urgency for developing effective treatment targets and prognostic biomarkers to improve the prognostic prediction and treatment outcomes of BRCA patients. This is conducive to identifying biomarkers with therapeutic benefits, constructing risk models to predict patients' disease worsening risks, and developing new therapeutic drugs. Necroptosis is triggered in response to the damage and resistance to apoptosis and acts as a tumor-suppressive process when a "failure" in apoptosis occurs. To our knowledge, evasion and resistance to apoptosis are crucial drivers of tumor development and drug resistance. Due to its dual effect, necroptosis also exerts a tumor-promoting effect. Currently, the prognostic mechanism for BRCA is unknown. Therefore, this study was performed to determine the risk signature of necroptosis-related miRNAs to predict the prognosis of BRCA patients.

The prognostic value and underlying regulatory mechanisms of 13 necroptosis-related miRNAs in BRCA were the main focus of this study. After characterizing the expression profiles of these miRNAs in BRCA patients and normal control samples, half of the miRNAs were identified as differentially expressed between tumor and non-tumor samples. Screening for differentially expressed miRNAs identified disease-related miRNAs. By performing Cox regression analysis, the risk signature of 6 necroptosis-related miRNAs was determined to assess its prognostic value in BRCA patients. Among the six necroptosis-related miRNAs identified in this study, miR-148a-3p and miR-7-5p were identified as potential risk factors, while miR-223-3p, miR-141-3p, miR-200a-5p, and miR-425-5p as protective factors. Further analysis showed that the risk signature based on the 6 necroptosis-related miRNAs was an independent predictor of OS and could distinguish low-risk patients from high-risk ones. Compared with clinical risk factors, this signature exhibits a superior prognostic value.

Nomogram is a visual tool that can be intuitively used to develop sensitive predictive models [21, 34]. Presently, nomogram has been extensively applied in various diseases, especially in cancer risk assessment, tumor relapse and metastasis prediction, and treatment efficacy evaluation [35–38]. However, few studies have integrated miRNA risk signature with clinicopathological characteristics, especially based on the risk signature of necroptosis-related miRNAs. Thus, this study integrated the risk signature of six necroptosis-related miRNAs with clinicopathological characteristics to construct a nomogram to provide personalized prognosis prediction for BRCA patients. The total nomogram score for each BRCA patient could be used to predict the 3- and 5-year overall survival. Compared with conventional evaluation tools (such as TNM staging), this nomogram was found to be significantly more accurate in predicting the OS of BRCA.

The protective factor of miR-223-3p was found to share the closest correlation with the OS of BRCA patients, and its low expression was correlated with poor prognosis. Functional analysis identified 30 potential target genes of miR-223-3p. KEGG analysis of these genes showed that the MAPK signaling pathway and signaling pathways regulating pluripotency of stem cells were the two most enriched pathways. Current studies have shown a close association of the MAPK signaling pathway with tumor proliferation, invasion and metastasis, as well as involvement in cell apoptosis and autophagy modulation [39–42]. BRCA stem cells, the main participants in tumor aggressiveness, contribute to the presence of drug resistance and invasion [43]. Thus, miR-223-3p, a protective factor, may impact the occurrence, metastasis, and drug resistance of BRCA and could potentially mediate the above-mentioned signaling pathways to limit the cancer initiation and progression and reverse drug resistance. However, the exact contribution of miR-223-3p to necroptosis in BRCA warrants more comprehensive and in-depth studies.

Although this present study comprehensively investigated the relationships among necroptosis, miRNAs, and the prognosis of BRCA patients, there were some limitations that should be addressed. First, all data were derived from retrospective datasets. Second, we analyzed data only through bioinformatics, which needs to be validated in large-scale clinical studies and *in vivo* and *in vitro* experiments. Lastly, we did not explore the prognostic risk signature for different types of molecular breast cancer.

5. Conclusions

We assessed the prognostic value of the miRNAs related to necroptosis in BRCA and formulated a risk signature that was found to be an independent prognostic factor for BRCA patients. miR-223-3p was identified as a protective factor for patients' survival and may have a key tumor-suppressive role in BRCA and antagonizing drug resistance. Additionally, the prognostic nomogram developed by combining the risk signature of necroptosis-related miRNAs and clinicopathological characteristics could effectively predict the clinical prognosis of BRCA patients, and could be used as an individualized predictive tool in clinical practice.

AUTHOR CONTRIBUTIONS

ZR and WS—designed the research study; XHH and GYW—performed the research; XHH, GYW and WS—analyzed the data; XHH, GYW and ZR—wrote the manuscript. All authors read and approved the final manuscript.

ETHICS APPROVAL AND CONSENT TO PARTICIPATE

Not applicable.

ACKNOWLEDGMENT

Not applicable.

FUNDING

This work was supported by Guangxi Key Cultivation discipline construction project of traditional Chinese Medicine (GZXK-P-20-07), Innovation Project of Guangxi Graduate Education (YCBZ2021077) and Guangxi Postdoctoral Special

fund project.

CONFLICT OF INTEREST

The authors declare no conflict of interest.

REFERENCES

[1] Nagini S. Breast cancer: current molecular therapeutic targets and new players. Anti-Cancer Agents in Medicinal Chemistry. 2017; 17: 152–163.

[2] Sung H, Ferlay J, Siegel RL, Laversanne M, Soerjomataram I, Jemal A, *et al*. Global cancer statistics 2020: GLOBOCAN estimates of incidence and mortality worldwide for 36 cancers in 185 countries. A Cancer Journal for Clinicians. 2021; 71: 209–249.

[3] Anderson WF, Katki HA, Rosenberg PS. Incidence of breast cancer in the United States: current and future trends. Journal of the National Cancer Institute. 2011; 103: 1397–1402.

[4] Anderson WF, Rosenberg PS, Petito L, Katki HA, Ejlertsen B, Ewertz M, *et al*. Divergent estrogen receptor-positive and -negative breast cancer trends and etiologic heterogeneity in Denmark. International Journal of Cancer. 2013; 133: 2201–2206.

[5] Mullooly M, Murphy J, Gierach GL, Walsh PM, Deady S, Barron TI, *et al*. Divergent oestrogen receptor-specific breast cancer trends in Ireland (2004–2013): amassing data from independent western populations provide etiologic clues. European Journal of Cancer. 2017; 86: 326–333.

[6] Joko-Fru WY, Miranda-Filho A, Soerjomataram I, Egue M, Akele-Akpo MT, N'da G, *et al*. Breast cancer survival in sub-Saharan Africa by age, stage at diagnosis and human development index: a population-based registry study. International Journal of Cancer. 2020; 146: 1208–1218.

[7] Nagini S. Breast cancer: current molecular therapeutic targets and new players. Anti-Cancer Agents in Medicinal Chemistry. 2017; 17: 152–163.

[8] Christofferson DE, Yuan J. Necroptosis as an alternative form of programmed cell death. Current Opinion in Cell Biology. 2010; 22: 263–268.

[9] Nikoletopoulou V, Markaki M, Palikaras K, Tavernarakis N. Crosstalk between apoptosis, necrosis and autophagy. Biochimica et Biophysica Acta. 2013; 1833: 3448–3459.

[10] Sun L, Wang H, Wang Z, He S, Chen S, Liao D, *et al*. Mixed lineage kinase domain-like protein mediates necrosis signaling downstream of RIP3 kinase. Cell. 2012; 148: 213–227.

[11] Tanzer M, Tripaydonis A, Webb A, Young S, Varghese L, Hall C, *et al*. Necroptosis signalling is tuned by phosphorylation of MLKL residues outside the pseudokinase domain activation loop. The Biochemical Journal. 2015; 471: 255–265.

[12] Liu Y, Chen Q, Zhu Y, Wang T, Ye L, Han L, *et al*. Non-coding RNAs in necroptosis, pyroptosis and ferroptosis in cancer metastasis. Cell Death Discovery. 2021; 7: 210.

[13] Höckendorf U, Yabal M, Herold T, Munkhbaatar E, Rott S, Jilg S, *et al*. RIPK3 restricts myeloid leukemogenesis by promoting cell death and differentiation of leukemia initiating cells. Cancer Cell. 2016; 30: 75–91.

[14] Shahsavari Z, Karami-Tehrani F, Salami S, Ghasemzadeh M. RIP1K and RIP3K provoked by shikonin induce cell cycle arrest in the triple negative breast cancer cell line, MDA-MB-468: necroptosis as a desperate programmed suicide pathway. Tumor Biology. 2016; 37: 4479–4491.

[15] Novohradsky V, Markova L, Kostrhunova H, Trávníček Z, Brabec V, Kasparkova J. An anticancer Os (II) bathophenanthroline complex as a human breast cancer stem cell-selective, mammosphere potent agent that kills cells by necroptosis. Scientific Reports. 2019; 9: 13327.

[16] Shen F, Pan X, Li M, Chen Y, Jiang Y, He J. Pharmacological inhibition of necroptosis promotes human breast cancer cell proliferation and metastasis. OncoTargets and Therapy. 2020; 13: 3165–3176.

[17] Hill M, Tran N. MiRNA interplay: mechanisms and consequences in cancer. Disease Models & Mechanisms. 2021; 14: 1–9.

[18] Liu B, Li J, Cairns MJ. Identifying miRNAs, targets and functions. Briefings in Bioinformatics. 2014; 15: 1–19.

[19] MacFarlane L, R. Murphy P. MicroRNA: biogenesis, function and role in cancer. Current Genomics. 2010; 11: 537–561.

[20] Hata A, Kashima R. Dysregulation of microRNA biogenesis machinery in cancer. Critical Reviews in Biochemistry and Molecular Biology. 2016; 51: 121–134.

[21] Yang Y, Qu A, Wu Q, Zhang X, Wang L, Li C, *et al*. Prognostic value of a hypoxia-related microRNA signature in patients with colorectal cancer. Aging. 2020; 12: 35–52.

[22] Lin S, Gregory RI. MicroRNA biogenesis pathways in cancer. Nature Reviews Cancer. 2015; 15: 321–333.

[23] Xu J, Wu KJ, Jia QJ, Ding XF. Roles of miRNA and lncRNA in triple-negative breast cancer. Journal of Zhejiang University-Science B. 2020;21: 673–689.

[24] Tang X, Hou Y, Yang G, Wang X, Tang S, Du Y, *et al*. Stromal miR-200s contribute to breast cancer cell invasion through CAF activation and ECM remodeling. Cell Death and Differentiation. 2016; 23: 132–145.

[25] Kong X, Li G, Yuan Y, He Y, Wu X, Zhang W, *et al*. MicroRNA-7 inhibits epithelial-to-mesenchymal transition and metastasis of breast cancer cells via targeting FAK expression. PLoS One. 2012; 7: e41523.

[26] Qian X, Xiao F, Chen Y, Yuan J, Liu X, Wang L, *et al*. Computerized assessment of the tumor-stromal ratio and proposal of a novel nomogram for predicting survival in invasive breast cancer. Journal of Cancer. 2021; 12: 3427–3438.

[27] Cao M, Cai J, Yuan Y, Shi Y, Wu H, Liu Q, *et al*. A four-gene signature-derived risk score for glioblastoma: prospects for prognostic and response predictive analyses. Cancer Biology & Medicine. 2019;16: 595–605.

[28] Zhao X, Cui L. A robust six-miRNA prognostic signature for head and neck squamous cell carcinoma. Journal of Cellular Physiology. 2020; 235: 8799–8811.

[29] Kamarudin AN, Cox T, Kolamunnage-Dona R. Time-dependent ROC curve analysis in medical research: current methods and applications. BMC Medical Research Methodology. 2017; 17: 53.

[30] Namdar K, Haider MA, Khalvati F. A modified AUC for training convolutional neural networks: taking confidence into account. Frontiers in Artificial Intelligence. 2021; 4: 582928.

[31] Yang Z, Lu S, Wang Y, Tang H, Wang B, Sun X, *et al*. A novel defined necroptosis-related miRNAs signature for predicting the prognosis of colon cancer. International Journal of General Medicine. 2022; 15: 555–565.

[32] Wu T, Hu E, Xu S, Chen M, Guo P, Dai Z, *et al*. ClusterProfiler 4.0: a universal enrichment tool for interpreting omics data. Innovation. 2021; 2: 100141.

[33] Jiang M, Li C, Pan C, Lv W, Ren Y, Cui X, *et al*. Nomogram for predicting transmural bowel infarction in patients with acute superior mesenteric venous thrombosis. World Journal of Gastroenterology. 2020; 26: 3800–3813.

[34] Balachandran VP, Gonen M, Smith JJ, DeMatteo RP. Nomograms in oncology: more than meets the eye. The Lancet Oncology. 2015; 16: e173–e180.

[35] Wu J, Zhang H, Li L, Hu M, Chen L, Xu B, *et al*. A nomogram for predicting overall survival in patients with low-grade endometrial stromal sarcoma: a population-based analysis. Cancer Communications. 2020; 40: 301–312.

[36] Zheng W, Li K, Zhu W, Ding Y, Wu Q, Tang Q, *et al*. Nomogram prediction of overall survival based on log odds of positive lymph nodes for patients with penile squamous cell carcinoma. Cancer Medicine. 2020; 9: 5425–5435.

[37] Zhang W, Fang M, Dong D, Wang X, Ke X, Zhang L, *et al*. Development and validation of a CT-based radiomic nomogram for preoperative prediction of early recurrence in advanced gastric cancer. Radiotherapy and Oncology. 2020; 145: 13–20.

[38] Wang W, Yang Z, Ouyang Q. A nomogram to predict skip metastasis in papillary thyroid cancer. World Journal of Surgical Oncology. 2020; 18: 167.

[39] Yang S, Liu G. Targeting the Ras/Raf/MEK/ERK pathway in hepatocellular carcinoma. Oncology Letters. 2017; 13: 1041–1047.

[40] Pandian J, Panneerpandian P, Devanandan HJ, Sekar BT, Balakrishnan K, Selvarasu K, *et al*. Identification of the targeted therapeutic potential of doxycycline for a subset of gastric cancer patients. Annals of the New York Academy of Sciences. 2020; 1467: 94–111.

[41] Provenzano PP, Inman DR, Eliceiri KW, Keely PJ. Matrix density-induced mechanoregulation of breast cell phenotype, signaling and gene expression through a FAK-ERK linkage. Oncogene. 2009; 28: 4326–

4343.
[42] Hung S, Chen W, Lee Y, Su J, Juan Y, Lin I, *et al*. Rhopaloic acid A induces apoptosis, autophagy and MAPK activation through ROS-mediated signaling in bladder cancer. Phytomedicine. 2021; 92: 153720.
[43] Barzaman K, Karami J, Zarei Z, Hosseinzadeh A, Kazemi MH, Moradi-Kalbolandi S, *et al*. Breast cancer: biology, biomarkers, and treatments. International Immunopharmacology. 2020; 84: 106535.

How to cite this article: Xiaohua Hong, Guangyao Wang, Zhen Rong, Wei Shi. A prognostic signature of six necroptosis-related miRNAs for predicting the overall survival of breast cancer patients. European Journal of Gynaecological Oncology. 2022; 43(6): 69-82. doi: 10.22514/ejgo.2022.060.